

A Node Elimination Algorithm for Cubature of High-Dimensional Polytopes^{*}

Arkadijs Slobodkins^a, Johannes Tausch^{a,*}

^a*Department of Mathematics, Southern Methodist University, Dallas, TX 75275, USA*

Abstract

Node elimination is a numerical approach to obtain cubature rules for the approximation of multivariate integrals. Beginning with a known cubature rule, nodes are selected for elimination, and a new, more efficient rule is constructed by iteratively solving the moment equations. This paper introduces a new criterion for selecting which nodes to eliminate that is based on a linearization of the moment equation. In addition, a penalized iterative solver is introduced, that ensures that weights are positive and nodes are inside the integration domain. A strategy for constructing an initial quadrature rule for various polytopes in several space dimensions is described. High efficiency rules are presented for two, three and four dimensional polytopes. The new rules are compared with rules that are obtained by combining tensor products of one dimensional quadrature rules and domain transformations, as well as with known analytically constructed cubature rules.

Keywords: Multivariate integration, Numerical cubature, Node elimination, Least squares Newton method, Constrained optimization.

1. Introduction

Let Ω be a domain in \mathbb{R}^d . The goal of the construction of cubature rules is to determine the nodes x_k and weights w_k in the cubature rule

$$\int_{\Omega} \phi(x) w(x) dx \approx \sum_{k=1}^n \phi(x_k) w_k, \quad (1)$$

such that the rule is exact for multivariate polynomials of degree up to p

$$\mathbb{P}_p^d = \text{span} \{x^\alpha : \alpha_1 + \cdots + \alpha_d \leq p\}.$$

^{*}This material is based upon work supported by the National Science Foundation under grant DMS-17207431.

^{*}Corresponding author

Email addresses: aslobodkins@smu.edu (Arkadijs Slobodkins), tausch@smu.edu (Johannes Tausch)

Here, α is a multi index and $x^\alpha = x_1^{\alpha_1} \cdots x_d^{\alpha_d}$. The dimension of the linear space \mathbb{P}_p^d is

$$M = \dim \mathbb{P}_p^d = \binom{p+d}{d}.$$

From the viewpoint of numerics the monomial basis is ill-conditioned, and so we consider a more general basis ϕ_1, \dots, ϕ_M of \mathbb{P}_p^d , for instance, orthogonal polynomials. We set

$$\Phi(x) = \begin{bmatrix} \phi_1(x) \\ \vdots \\ \phi_M(x) \end{bmatrix}, \quad \mathbf{b} = \begin{bmatrix} \int_{\Omega} \phi_1(x) w(x) dx \\ \vdots \\ \int_{\Omega} \phi_M(x) w(x) dx \end{bmatrix}. \quad (2)$$

Further, we write for the vector of nodes and weights, $\mathbf{x} \in \mathbb{R}^{dn}$, $\mathbf{w} \in \mathbb{R}^n$, respectively, and

$$\Phi(\mathbf{x}) = [\Phi(x_1), \dots, \Phi(x_n)] \in \mathbb{R}^{M \times n}. \quad (3)$$

Exactness in \mathbb{P}_p^d means that the nodes and weights must be solutions of moment equations

$$\mathbf{f}(\mathbf{x}, \mathbf{w}) = \Phi(\mathbf{x})\mathbf{w} - \mathbf{b} = \mathbf{0}. \quad (4)$$

which is a polynomial system in $N = (d+1)n$ unknowns and M equations. We write (4) in more convenient form by combining nodes and weights into one vector. Thus we let

$$z_k = [x_k, w_k] \in \mathbb{R}^{d+1} \quad \text{and} \quad \mathbf{z} = [z_1, \dots, z_n]^T \in \mathbb{R}^N. \quad (5)$$

Since we are looking for nodes in the domain Ω that have positive weights, a feasible cubature rule is in the set

$$Z_n = \{\mathbf{z} \in \mathbb{R}^N : \mathbf{f}(\mathbf{z}) = \mathbf{0}, x_k \in \Omega, w_k \geq 0, 1 \leq k \leq n\}.$$

A solution of (4) in Z_n is said to have quality PI, which means that all weights are positive and all nodes are inside the domain. The construction of cubature rules has considerable interest in several application areas. For instance, rules for three dimensional polytopes are used in the p -version of the finite element method [2]. The Galerkin boundary element method involves integrals over four dimensional polytopes [13, 17, 11]. Likewise, variational formulations of elliptic fractional PDEs in two or three dimensions lead to four or six-dimensional integrals [3].

Since (4) is a polynomial system, it can be approached from the perspective of algebraic geometry, see [4] and the reference therein. In principle, the system can be solved using Gröbner bases and Buchberger's algorithm. However, the computational complexity of these algorithms grows very quickly with the number of variables, so that in practice the method can only provide solutions for relatively low degree and dimension. In addition, surprisingly little is known about the solvability of (4). In particular, the smallest value of n for which Z_n is non-empty is generally unknown.

One can expect that the solutions of (4) live on higher dimensional algebraic varieties if the system is underdetermined, i.e., N is greater than M . If $N = M$ the solutions are isolated points. This however, does not preclude that there are rules with fewer nodes. We call a rule optimal, if n is the smallest integer such that $N \geq M$. For a collection of cubature rules that were derived using analytic means we refer to [5].

To illustrate the issues with multidimensional cubature, consider the case that Ω is a hypercube. In this case cubature rules can be easily found by forming tensor products of one-dimensional Gauss quadrature rules. The resulting rules are solutions of (4), but these rules become highly underdetermined as the degree and the dimension is increased.

For larger values of p and d , analytical methods for constructing solutions become very difficult, if not impossible, and therefore methods that solve (4) with Newton-like methods and/or stochastic methods have been researched extensively in the recent years, see, e.g., [8, 16, 7, 9, 18].

In this article we focus on generating quadrature rules by node elimination, a technique that was initiated in the paper by Xiao and Gimbutas [19]. The idea is to begin with a known overdetermined rule and select a node for elimination from the rule. The reduced rule does not satisfy the moment equations, but is used as an initial guess for solving this nonlinear system by the Gauss-Newton iteration. The procedure is repeated until no further nodes can be eliminated.

Since nonlinear solvers typically converge only locally, the success of such an approach strongly depends on how a node is selected for elimination. Xiao and Gimbutas choose the node whose corresponding column in (3) has the smallest Euclidean norm (scaled by the weight). In this paper we present a new elimination criterion which is based on the linearization of the function $\mathbf{f}(\mathbf{x}, \mathbf{w})$ with the goal to guarantee a close initial guess for the nonlinear solver. Thus our node elimination procedure can be viewed as a predictor-corrector type method that is used in path following algorithms, see [1].

Another important aspect of node elimination is that a solution is only a useful cubature rule if the nodes are in Ω and the weights are positive. In this article we describe a new penalized optimization method that guarantees that nodes remain in the domain and have positive weights.

The outline of the remainder of this paper is as follows. In section 2 we describe the corrector step, which is a constrained least squares Newton method. In section 3 we discuss the improved node elimination step (predictor). One important aspect of node elimination is to come up with a good initial cubature rule. In section 4 we describe how this can be done for a variety of domains Ω . Finally, in section 5, we present some cubature rules that we found with the method. The codes of our node elimination scheme and some of the cubature rules that we obtained can be found on Github [14].

2. Penalized Least Squares Newton Method

As we already mentioned, the node elimination procedure is a predictor-corrector type method. In this section we describe the corrector step, which,

for a point $\tilde{\mathbf{z}} \notin Z_n$, attempts to find a nearby point on the solution manifold, i.e., $\bar{\mathbf{z}} \in Z_n$.

Since the goal is to obtain quadrature rules with nodes in the domain that have positive weights, we enforce these constraints by adding a penalty term. With \mathbf{z} defined as in (5), we set

$$\phi_\Omega(\mathbf{z}) = \sum_{j=1}^n \left[\varphi_\Omega(x_j) + \log \left(\frac{1}{w_j} \right) \right], \quad (6)$$

where $\varphi_\Omega(\cdot)$ is a function that is smooth in Ω and has a logarithmic singularity on the boundary of Ω . For instance, if Ω is a convex polytope given by the linear inequalities, then we set

$$\Omega = \{x \in \mathbb{R}^d : Ax \leq b\} \Rightarrow \varphi_\Omega(x) = \sum_{\ell=1}^{\ell_A} \log \left(\frac{1}{b_\ell - a_\ell^T x} \right),$$

where a_ℓ^T are the rows of A and ℓ_A is the number of rows. For the case of a sphere the penalty term is

$$\Omega = \{x \in \mathbb{R}^d : \|x\|_2 \leq 1\} \Rightarrow \varphi_\Omega(x) = \log \left(\frac{1}{1 - \|x\|_2} \right).$$

To derive an iterative solver that maps $\tilde{\mathbf{z}} \notin Z_n$ to $\bar{\mathbf{z}} \in Z_n$ let $\Delta\mathbf{z} = \tilde{\mathbf{z}} - \bar{\mathbf{z}}$, and consider the constrained optimization problem

$$\min_{\Delta\mathbf{z}} \left\{ \frac{1}{2} \|\Delta\mathbf{z}\|^2 + t \phi_\Omega(\tilde{\mathbf{z}} + \Delta\mathbf{z}), \tilde{\mathbf{z}} + \Delta\mathbf{z} \in Z_n \right\}. \quad (7)$$

Here, the parameter $t \geq 0$ controls the strength of the penalty term. We will provide more detail about how to determine t later on.

Now linearize (7) as follows

$$\begin{aligned} \min \quad & \frac{1}{2} \|\Delta\mathbf{z}\|^2 + t \mathbf{g}^T \Delta\mathbf{z} \\ \Delta\mathbf{z} : \quad & \mathbf{f}(\tilde{\mathbf{z}}) + J\Delta\mathbf{z} = \mathbf{0}, \end{aligned} \quad (8)$$

where $\mathbf{f} := \mathbf{f}(\tilde{\mathbf{z}}) \in \mathbb{R}^M$, $J := D\mathbf{f}(\tilde{\mathbf{z}}) \in \mathbb{R}^{M \times N}$ is the Jacobian of $\mathbf{f}(\tilde{\mathbf{z}})$ and $\mathbf{g} := \nabla\phi_\Omega(\tilde{\mathbf{z}}) \in \mathbb{R}^N$ is the gradient of the penalty term. Using Lagrange multipliers it follows that (8) is equivalent to the linear system

$$\begin{aligned} \Delta\mathbf{z} + J^T \boldsymbol{\lambda} &= -t\mathbf{g} \\ J\Delta\mathbf{z} &= -\mathbf{f} \end{aligned}$$

where $\boldsymbol{\lambda} \in \mathbb{R}^M$ is the Lagrange multiplier. Eliminating $\boldsymbol{\lambda}$ gives the solution of (8) in the the normal equations form

$$\begin{aligned} \Delta\mathbf{z} &= -J^T (JJ^T)^{-1} \mathbf{f} - t \left(I - J^T (JJ^T)^{-1} J \right) \mathbf{g} \\ &= \Delta\mathbf{z}^f + t\Delta\mathbf{z}^g. \end{aligned} \quad (9)$$

Here, $\Delta \mathbf{z}^f = -J^T (JJ^T)^{-1} \mathbf{f}$ is the least squares solution of the underdetermined system $\mathbf{f} + J\Delta \mathbf{z} = \mathbf{0}$, i.e., the solution of (7) when $t = 0$. The second term $\Delta \mathbf{z}^g = -\left(I - J^T (JJ^T)^{-1} J\right) \mathbf{g}$ is the orthogonal projection of $-\mathbf{g}$ onto the nullspace of J . The form in (9) makes clear that the solution of (8) for any parameter t can be obtained by computing $\Delta \mathbf{z}^f$ and $\Delta \mathbf{z}^g$ independently of t and then forming the appropriate linear combination.

For numerical purposes it is better to compute these two vectors with the LQ factorization. If $J = LQ$ is the economy size factorization, i.e., $L \in \mathbb{R}^{M \times M}$ is lower triangular and $Q \in \mathbb{R}^{M \times N}$ has orthonormal rows, then

$$\begin{aligned}\Delta \mathbf{z}^f &= -Q^T L^{-1} \mathbf{f}, \\ \Delta \mathbf{z}^g &= -(I - Q^T Q) \mathbf{g}.\end{aligned}\tag{10}$$

Once $\Delta \mathbf{z}^f$ and $\Delta \mathbf{z}^g$ have been computed, the Newton update is

$$\tilde{\mathbf{z}} \leftarrow \tilde{\mathbf{z}} + \Delta \mathbf{z}^f + t \Delta \mathbf{z}^g.\tag{11}$$

We now describe how the parameter t is determined. It is determined such that the nodes of next iterate have maximal distance from the boundary and weights are as large as possible. We focus on the case that Ω is a convex polytope given by the linear inequalities $Ax \leq b$.

Substitution of the j -th node and weight of the Newton update (11) into the linear constraints results in two types of inequalities

$$\begin{aligned}b_\ell - a_\ell^T (\tilde{x}_j + \Delta x_j^f) - t a_\ell^T \Delta x_j^g &\leq 0 \\ -\tilde{w}_j + \Delta w_j^f + t \Delta w_j^g &\leq 0\end{aligned}$$

for $1 \leq j \leq n$, $1 \leq \ell \leq \ell_A$. Here \tilde{x}_j , Δx_j^f and Δx_j^g are the nodal components and \tilde{w}_j , Δw_j^f and Δw_j^g are the weights of the vectors $\tilde{\mathbf{z}}$, $\Delta \mathbf{z}^f$ and $\Delta \mathbf{z}^g$, respectively. We write these conditions collectively as

$$m_k(t) = \beta_k + t \alpha_k \leq 0, \quad 1 \leq k \leq (\ell_A + 1)n,\tag{12}$$

where the α_k 's list all inner products $a_\ell^T \Delta x_j^g$ and all Δw_j^f 's and the β_k 's are defined analogously.

Algorithm 1 finds the value of t that minimizes the maximum over k for this family of straight lines. The algorithm starts with the maximum at $t = 0$ and follows the largest line until it intersects with another line with positive slope.

If successful, the algorithm returns the t -value for which the min max of the family of straight lines is achieved. This guarantees that the next iterate has maximal distance from the boundary. Note that even though $\tilde{\mathbf{z}}$ satisfies the constraints, the least squares solution $\tilde{\mathbf{z}} + \Delta \mathbf{z}^f$ may not. Therefore, it is possible that the returned value of $m_k(t)$ is positive in which case at least one node does not satisfy the constraints. In the latter case one can resort to a damped Newton method, where $\Delta \mathbf{z}^f$ is multiplied by a small factor. The theoretical cost

Algorithm 1 Determines the min max of the family of straight lines in (12). Here, t_{jk} denotes the intersection point of line m_j with m_k .

```

 $t = 0$ 
 $k = \operatorname{argmax}_j \beta_j$ 
while  $\alpha_k < 0$  do
    Find  $k^* = \operatorname{argmin}_k \{t_{jk}, t_{jk} > t\}$ 
     $t = t_{k^*k}$ 
     $k^* = k$ 
end while

```

of this algorithm is $O(\ell_A^2 n^2)$. However, in practice, the while loop terminates after a small number of steps, thus its computational cost is closer to $O(\ell_A n)$ and negligible compared to the cost of computing the LQ factorization of the matrix J .

We have described algorithm 1 for a convex polytope. However, it can be modified for other integration domains as well. For instance, if Ω is a solid sphere, then the constraints result in a family of parabolas and a completely analogous algorithm can be applied to optimize the parameter t .

The constrained LS Newton method is summarized in algorithm 2.

Algorithm 2 Maps $\tilde{\mathbf{z}}$ on a nearby point $\bar{\mathbf{z}}$ on Z_n .

```

while  $\|f(\tilde{\mathbf{z}})\| > TOL$  do
    Setup  $\mathbf{f}$ ,  $\mathbf{g}$  and  $J$ , and compute the LQ-factorization of  $J$ .
    Calculate  $\Delta \mathbf{z}^f$  and  $\Delta \mathbf{z}^g$  in (10).
    Determine  $t$  from algorithm 1.
    Set  $\tilde{\mathbf{z}} \leftarrow \tilde{\mathbf{z}} + \Delta \mathbf{z}^f + t \Delta \mathbf{z}^g$ 
end while

```

3. Node Elimination

In this section we describe a method to reduce the number of points in a cubature rule while maintaining its degree. It consists of determining points on Z_n that intersect with the coordinate planes $w_k = 0$. Obviously, if a weight vanishes in (1), then the corresponding node does not have to be included in the cubature rule (1). Thus we have found another solution of (4) with $n - 1$ nodes that has the same degree of precision. The elimination procedure is then repeated until no further quadrature rules with vanishing nodes can be found.

We start with a point $\bar{\mathbf{z}}$ on Z with positive weights and use a predictor-corrector type approach to find another point on Z_n where one of the w_k 's vanishes. The predictor step consists of linearizing \mathbf{f} at $\bar{\mathbf{z}}$ and then computing the nearest points on the tangent space that intersect with the one of the hyperplanes $w_k = 0$. The k -th node is then eliminated and the point $\tilde{\mathbf{z}}$ is mapped

to Z_{n-1} using algorithm 2. The predictor-corrector method is restarted to eliminate further nodes. This approach guarantees that all nodes remain in the domain and all weights are non-negative.

We now describe the predictor step in more detail. To obtain the tangent space of Z_n at $\bar{\mathbf{z}}$ consider the linearization of the function \mathbf{f} at $\bar{\mathbf{z}}$

$$\mathbf{f}(\bar{\mathbf{z}} + \Delta\mathbf{z}) = \mathbf{f}(\bar{\mathbf{z}}) + J\Delta\mathbf{z} + \mathcal{O}(|\Delta\mathbf{z}|^2),$$

where $J = D\mathbf{f}(\bar{\mathbf{z}})$. Since the first term on the right hand side vanishes, the tangent space is defined by $\mathbf{z} = \bar{\mathbf{z}} + \Delta\mathbf{z}$, where $\Delta\mathbf{z} \in \text{Null}(J)$. Since the matrix J is underdetermined, this nullspace is nontrivial. An orthonormal basis can be found with the full LQ-factorization of J

$$J = \begin{bmatrix} L, 0 \end{bmatrix} \begin{bmatrix} \tilde{Q} \\ \hat{Q} \end{bmatrix} \quad (13)$$

where $L \in \mathbb{R}^{M \times M}$ is lower triangular, $\tilde{Q} \in \mathbb{R}^{M \times N}$ and $\hat{Q} \in \mathbb{R}^{N-M \times N}$. The rows of \hat{Q} form an orthogonal basis of $\text{Null}(J)$.

To eliminate the k -th node, consider the nearest point $\tilde{\mathbf{z}}$ in the intersection of the tangent space with the hyperplane $w_k = 0$. If $\tilde{\mathbf{z}} = \bar{\mathbf{z}} + \Delta\mathbf{z}$ then $\Delta\mathbf{z}$ solves the optimization problem

$$\begin{aligned} \min \quad & \frac{1}{2} \|\Delta\mathbf{z}\|^2 + t \mathbf{g}^T \Delta\mathbf{z} \\ \Delta\mathbf{z} : \quad & J\Delta\mathbf{z} = \mathbf{0} \\ & w_k + \Delta w_k = 0. \end{aligned}$$

Here $\mathbf{g} = \nabla \phi_{\Omega,k}(\bar{\mathbf{z}})$, where $\phi_{\Omega,k}(\cdot)$ is the penalty function that is obtained by excluding the node k in the summation in equation (6).

The unknown $\Delta\mathbf{z}$ can be expressed as a combination of the orthogonal basis of $\text{Null}(J)$ obtained from the LQ factorization in (13). Thus there is a vector $\Delta\mathbf{y} \in \mathbb{R}^{N-M}$ such that $\Delta\mathbf{z} = \hat{Q}^T \Delta\mathbf{y}$. Substitution of this vector leads to the optimization problem

$$\begin{aligned} \min \quad & \frac{1}{2} \|\Delta\mathbf{y}\|^2 + t \hat{\mathbf{g}}^T \Delta\mathbf{y} \\ \Delta\mathbf{y} : \quad & \mathbf{m}_k^T \Delta\mathbf{y} = -\bar{w}_k. \end{aligned}$$

Here \mathbf{m}_k is the column of \hat{Q} corresponding to the k -th weight, and $\hat{\mathbf{g}}_k = \hat{Q}\mathbf{g}$. It can be seen that the solution $\Delta\mathbf{y}_k$ of the above optimization problem is given by

$$\Delta\mathbf{y}_k = \Delta\mathbf{y}_k^f + t\Delta\mathbf{y}_k^g, \quad (14)$$

where

$$\begin{aligned} \Delta\mathbf{y}_k^f &= \mathbf{m}_k \frac{\bar{w}_k}{\|\mathbf{m}_k\|^2} \\ \Delta\mathbf{y}_k^g &= \left(I - \frac{\mathbf{m}_k \mathbf{m}_k^T}{\|\mathbf{m}_k\|^2} \right) \hat{\mathbf{g}}, \end{aligned}$$

and thus the predictor is

$$\tilde{\mathbf{z}}_k = \bar{\mathbf{z}} + \Delta\mathbf{z}_k^f + t\Delta\mathbf{z}_k^g,$$

where $\Delta\mathbf{z}^f = \hat{Q}^T \Delta\mathbf{y}_k^f$ and $\Delta\mathbf{z}^g = \hat{Q}^T \Delta\mathbf{y}_k^g$. The parameter t is selected to ensure maximal distance from the domain boundary. If the domain Ω is a polytope, then this can be achieved with algorithm 1.

We compute in a list predictors $\tilde{\mathbf{z}}_k$ for all weights $k \in \{1, \dots, n\}$. The predictors that satisfy the constraints and are close to $\bar{\mathbf{z}}$ will be mapped on Z_{n-1} . The next quadrature is the solution that has the greatest distance from the boundary. The node elimination procedure is summarized in algorithm 3.

Algorithm 3 Node elimination algorithm.

```

Find a suitable initial cubature rule  $\bar{\mathbf{z}}$ .
while  $N > M$  do
    Setup  $J$ , and compute the LQ-factorization.
    for  $k=1:n$  do
        Compute  $\Delta\mathbf{z}_k^f$  and  $\Delta\mathbf{z}_k^g$  in (3).
        Compute  $t$  using algorithm 1.
        Set  $\Delta\mathbf{z}_k = \Delta\mathbf{z}_k^f + t\Delta\mathbf{z}_k^g$  and  $\tilde{\mathbf{z}}_k = \bar{\mathbf{z}}_k + \Delta\mathbf{z}_k$ .
    end for
    Sort the  $\Delta\mathbf{z}_k$ 's that satisfy the constraints such that
         $\|\Delta\mathbf{z}_1\| \leq \|\Delta\mathbf{z}_2\| \leq \dots$ 

    for  $k=1:K$  do
        Eliminate the  $k$ -th node from  $\tilde{\mathbf{z}}_k$ .
        Use algorithm 2 to map  $\tilde{\mathbf{z}}_k$  to  $\bar{\mathbf{z}}_k \in Z_{n-1}$ 
    end for
    Stop if no  $\bar{\mathbf{z}}_k \in Z_{n-1}$  could be found.
     $\bar{\mathbf{z}} \leftarrow \bar{\mathbf{z}}_k$ , where  $\bar{\mathbf{z}}_k$ 's nodes have the greatest distance from the boundary.
     $n \leftarrow n - 1$ 
end while

```

The main cost in this algorithm is to set up Jacobians and compute their QR factorizations.

4. Strategies for the Initial Cubatures

The discussion so far assumed that an initial cubature rule is known which may be suboptimal (i.e., it has more nodes than necessary), but has the desired degree. This section describes how such an initial cubature can be obtained. Here the goal is to keep the number of nodes low such that fewer elimination steps have to be taken and the cost of the linear algebra in the initial stages of the algorithm is reduced.

The scheme is based on the fact that cubature rules for Cartesian product domains $\Omega = \Omega_1 \times \Omega_2$ can be obtained by forming tensor products of cubature

rules of Ω_1 and Ω_2 . Specifically, if $\{\mathbf{x}_n, w_n\}$ and $\{\mathbf{y}_m, v_m\}$ are cubature rules for Ω_1 and Ω_2 that are exact for $\mathbb{P}_p^{d_1}$ and $\mathbb{P}_p^{d_2}$, respectively, then $\{(\mathbf{x}_n, \mathbf{y}_m), w_n v_m\}$ is a cubature rule that is exact for $\mathbb{P}_p^{d_1} \times \mathbb{P}_p^{d_2}$. Since this polynomial space is larger than $\mathbb{P}_p^{d_1+d_2}$, the node elimination can be performed with the tensor product rule as an initial guess.

We start the discussion with the case that Ω is the d -dimensional unit cube

$$C_d = \{(x_1, \dots, x_d) : 0 \leq x_i \leq 1, i = 1, \dots, d\}.$$

If one were to use tensor products of degree- p Gauss Legendre rules as the initial quadrature, one would obtain $(\lfloor p/2 \rfloor + 1)^d$ nodes. The rapid growth of this number makes this strategy unfeasible even for moderate values of p and d .

Instead, our implementation uses an iterative scheme to obtain the initial guess for the domains of interest, thereby significantly decreasing the initial number of nodes. We build the rule incrementally, by starting with $C_1 \times C_1$, and running node elimination. The resulting rule is then tensored with the C_1 -rule to obtain an initial guess for C_3 . The scheme is repeated until the desired dimension is reached. With this approach the number of nodes of the initial guess in the last step is greatly reduced over a d -fold tensor product of rules for C_1 .

We now turn to the d -dimensional simplex

$$T_d = \{(x_1, \dots, x_d) : 0 \leq x_d \leq \dots \leq x_1 \leq 1\}$$

and to Cartesian products of cubes and simplices.

The well known Duffy transformation can be used to transform a cube into a simplex. For the $d + 1$ -dimensional simplex it can be defined recursively as follows

$$\begin{aligned} x_1 &= \xi, \\ x_2 &= \xi \eta_1, \\ x_3 &= \xi \eta_2, \\ &\vdots \\ x_{d+1} &= \xi \eta_d. \end{aligned} \tag{15}$$

Here $\xi \in [0, 1] = C_1$ and $\boldsymbol{\eta} = (\eta_1, \dots, \eta_d) \in T_d$. Thus (15) transforms $C_1 \times T_d$ into T_{d+1} with Jacobian $J = \xi^d$. Now T_d can be transformed with another Duffy transform and repeating this leads to a transformation from C_{d+1} to T_{d+1} . However, for the construction of initial quadrature rules it is more convenient to work with one transformation at a time.

For instance, for the triangle (i.e. $d = 1$), we use Gauss-Jacobi rules for the integral over the (ξ, η) variables. Specifically, if

$$\int_0^1 f(\eta) d\eta \approx \sum_{\ell=1}^q f(y_\ell) v_\ell \quad \text{and} \quad \int_0^1 f(\xi) \xi d\xi \approx \sum_{k=1}^q f(x_k) w_k$$

are the quadrature rules of degree $p = 2q - 1$ for weight function $w(\eta) = 1$ and $w(\xi) = \xi$, respectively, then an integral over T_2 can be approximated as follows

$$\int_{T_2} \varphi(\mathbf{x}) d\mathbf{x} = \int_0^1 \int_0^1 \varphi(\xi, \xi\eta) \xi d\eta d\xi \approx \sum_{\substack{k=1 \\ \ell=1}}^p \varphi(x_k, x_k y_\ell) w_k v_\ell. \quad (16)$$

Note that the Jacobian ξ determines the choice of rule and affects the nodes x_k and weights w_k . If $\varphi \in \mathbb{P}_p^2$, then $(\xi, \eta) \mapsto \varphi(\xi, \xi\eta)$ is a polynomial in $\mathbb{P}_p^1 \times \mathbb{P}_p^1$ and thus the quadrature rule (16) is exact. This tensor product rule can now be used as the initial rule in the node-elimination procedure.

Similar to the cube, the $d + 1$ -dimensional simplex rule is built by recursion using previously generated rules. Thus, if $\{\mathbf{x}_k, w_k\}$ is a degree- p Gauss-Jacobi rule for $\int_0^1 f(\xi) \xi^d d\xi$ and $\{\mathbf{y}_l, v_l\}$ is a degree- p rule for T_d , then

$$\int_{T_{d+1}} \varphi(\mathbf{x}) d\mathbf{x} = \int_0^1 \int_{T_d} \varphi(\xi, \xi\mathbf{\eta}) \xi^d d\mathbf{\eta} d\xi \approx \sum_{k,l} \varphi(x_k, x_k \mathbf{y}_l) w_k v_l$$

is a degree- p rule for T_{d+1} .

For tensor products of cubes and simplices the analogous procedures can be applied, where some care must be taken to use the appropriate Gauss-Jacobi rule to compensate for the Jacobian of the Duffy transformation.

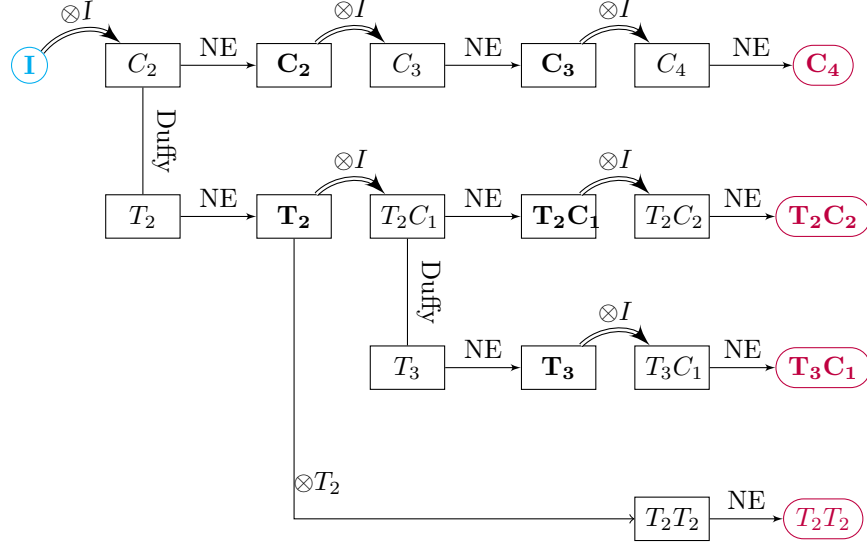


Figure 1: Construction scheme for quadrature rules for the four dimensional polytopes C_4 , $T_2 \times C_2$, $T_3 \times C_1$, $T_2 \times T_2$

Figure 1 illustrates the procedure for various polytopes in four dimensions. It begins with Gaussian cubature on the interval (shown in blue). Then the

tensor product of Gaussian quadrature on $I \otimes I$ is applied, which is an initial guess for C_2 . Subsequently, depending on the domain of interest, we either proceed by running the Node Elimination algorithm, or applying the Duffy transformation to obtain T_2 . Figure 1 describes how to derive initial guesses for C_4 , $T_2 \times C_2$, $T_3 \times C_1$ and $T_2 \times T_2$, before performing the final node elimination step, which is shown in red.

5. Numerical Examples

We have implemented the method in C++ using double precision arithmetic and the LAPACKE interface to the multithreaded implementation of LAPACK library for the dense linear algebra. The tests were run on a single process of a standard desktop system with an Intel I7 processor and 32 gigabyte of memory. All shown examples could be run with much less memory usage than our system had.

For the basis functions in (2) we use tensor products of Legendre polynomials for the cubes and the orthogonal triangular polynomials in [10]. The construction in this paper can be extended to obtain orthogonal polynomials for simplices of any dimension, which we implemented in our code.

The number of iterations in the corrector step is always small. Throughout most of the node elimination algorithm, the corrector converges after one to three iterations. Only in the final stages, when the system is less overdetermined, the typical number of iterations increases to three to seven, in rare cases up to ten. The elimination procedure is stopped if either the optimal number of nodes has been reached or if algorithm 1 is unable to find a value of t for all predictors. The tolerance in algorithm 2 is $TOL = 10^{-14}$.

Table 1 displays data about the final cubature rules obtained with our node elimination algorithm for the domain T_2 . Here n_{tp} is the number of points in the tensor product rule (16), which is the initial cubature rule, and n_{elim} is the number of points in the final rule. The optimal number of nodes and the efficiency ratio is given by

$$n_{opt} = \left\lceil \frac{\dim \mathbb{P}_p^d}{(d+1)} \right\rceil \quad \text{and} \quad i_{opt} = \frac{n_{opt}}{n_{elim}}.$$

The table contains only odd degree rules, because there are no even degree tensor product rules. Even degree rules could have been easily obtained by starting with the next degree odd tensor product rule, and enforcing only the even degree in the moment equations.

One can see that our algorithm found rules that are very close to optimal. One should note that rules for T_2 of similar quality have been obtained by other authors, including [19].

Our implementation does not exploit or enforce any symmetry, therefore the computed rules are in general not symmetric. Figure 2 displays for some examples the location of the nodes and size of the weights, indicated by the radius of the circles. For the figure, we have mapped T_2 to an equilateral

degree	3	5	7	9	11	13	15
n_{tp}	4	9	16	25	36	49	64
n_{elim}	4	7	12	19	27	38	47
n_{opt}	4	7	12	19	26	35	46
i_{opt}	1.00	1.00	1.00	1.00	0.96	0.92	0.98

degree	17	19	21	23	25	27	29
n_{tp}	81	100	121	144	169	196	225
n_{elim}	58	74	86	102	119	142	163
n_{opt}	57	70	85	100	117	136	155
i_{opt}	0.98	0.94	0.99	0.98	0.98	0.96	0.95

Table 1: Data for the cubature rules on the triangle

triangle to better assess the symmetries of the nodes. The rule of degree five is fully symmetric and is identical to a rule that has been found by analytical methods, see [15]. It is also the only rule we found where $M = N$ in the moment equations. This implies that the solution is an isolated point, and it makes sense to calculate the difference of the analytic solution with the numerically obtained one. We have found that the maximal difference is $1.14 \cdot 10^{-16}$, which is well within machine precision.

The rule of degree seven only has the three rotational symmetries, but none of the reflectional symmetries of the equilateral triangle. The rule of degree nine is symmetric up to seven digits of accuracy. The nearby symmetric version is known, see Dunavant [6]. Both rules solve the moment equations to machine precision. Note that while this rule is optimal, the moment equations are still underdetermined, because $N = 3 \cdot 19 = 57$ and $M = \frac{1}{2} \cdot 10 \cdot 11 = 55$. Thus our rule and Dunavant's rule are nearby solutions on a two dimensional manifold.

The higher degree rules in table 1 are not symmetric, but the nodes are generally following a symmetric distribution and the weights tend to be larger in the interior of the domain. This happens despite the fact that the nodes of the initial rules are more concentrated near the origin.

For the lower degree rules it can be determined analytically whether and how many fully symmetric rules exist, see [12]. Thus it is interesting to compare the theoretically predicted PI rules with those we obtained in table 1. In addition to the already mentioned degree five and nine rules, the paper [12] states that there are four fully symmetric PI rules of degree 11 with 30 nodes, and two rules of degree 13 with 37 points and one rule of degree 15. Our degree 11 rule has fewer nodes but is not symmetric, while the degree 13 rule has one more node and the degree 15 rule has the same number of nodes, albeit no symmetries. There is no symmetric PI rule of degree 7, but our algorithm was able to find an optimal rule with partial symmetry.

The results for the domain T_3 are shown in table 2. The encyclopedia of cubature rules [5] lists a PI rule of degree 6 with 29 nodes, and higher degree

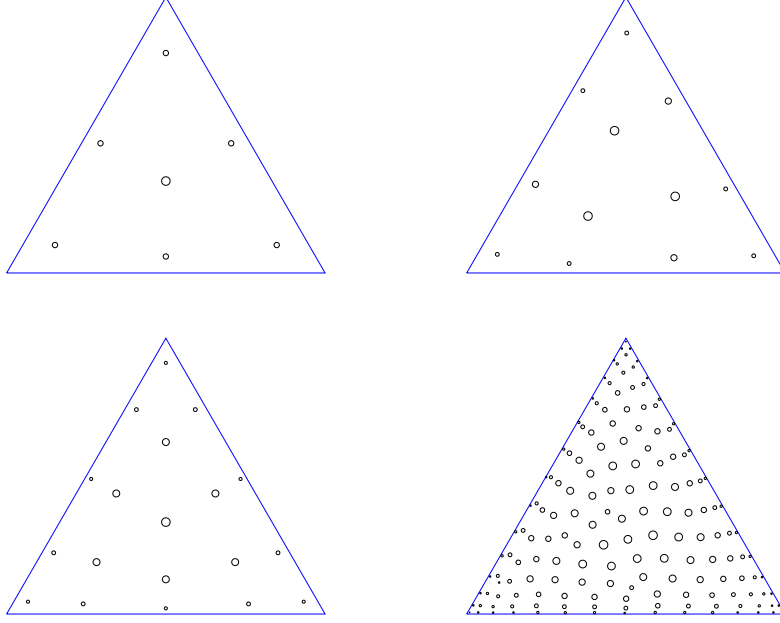


Figure 2: Quadrature nodes for a triangle. The degrees are 5, 7, 9 and 29.

rules with indefinite weights. The paper [8] reports a numerically generated rule of degree 19 with 392 and a rule of degree 20 with 448 nodes.

Finally, tables 3 and 4 show the data of the numerically computed rules for the four dimensional domains T_4 and $T_2 \times T_2$. For comparison, the highest PI T_4 -quadrature rule in [5] has degree five and 31 nodes.

The quadrature rules can be found in the git-hub repository [14].

degree	5	7	9	11	13	15	17	19	21	23
n_{tp}	27	64	125	216	343	512	729	1000	1331	1728
n_{elim}	14	31	57	95	143	206	288	390	510	653
n_{opt}	14	30	55	91	140	204	285	385	506	650
i_{opt}	1.00	0.97	0.96	0.96	0.98	0.99	0.99	0.99	0.99	0.99

Table 2: Data for the cubature rules on the 3D simplex

degree	3	5	7	9	11	13	15
n_{tp}	16	81	256	625	1296	2401	4096
n_{elim}	8	26	68	150	283	497	787
n_{opt}	7	26	66	143	273	476	776
i_{opt}	0.88	1.00	0.97	0.95	0.96	0.96	0.99

Table 3: Data for the cubature rules for T_4 .

degree	3	5	7	9	11	13	15
n_{tp}	16	81	256	625	1296	2401	4096
n_{elim}	8	26	67	146	277	478	781
n_{opt}	7	26	66	143	273	476	776
i_{opt}	0.88	1.00	0.99	0.98	0.99	0.99	0.99

Table 4: Data for the cubature rules for $T_2 \times T_2$.

Quadrature errors

To test the cubature rules over the simplices we consider the integral

$$I = \int_{\Omega} \frac{\exp(\mathbf{a}^T \mathbf{x}) - 1}{\mathbf{a}^T \mathbf{x}} d\mathbf{x} \quad (17)$$

where $\Omega \in \{T_2, T_3, T_4, T_2 \times T_2\}$. Note that the integrand is an analytic function in all variables, even if $\mathbf{a}^T \mathbf{x}$ vanishes. The vector \mathbf{a} is chosen randomly from the hypercube $[-25, 25]^d / \sqrt{d}$, where d is the dimension of Ω . To compute the reference value we express the integrand in form of an additional integral, which is computed numerically. Thus

$$I = \int_0^1 \int_{\Omega} \exp(t \mathbf{a}^T \mathbf{x}) d\mathbf{x} dt \approx \sum_k \int_{\Omega} \exp(t_k \mathbf{a}^T \mathbf{x}) d\mathbf{x} w_k, \quad (18)$$

where t_k, w_k are the Gauss-Legendre points. The integral in (18) over the exponential function can be determined analytically for the considered domains and we use a quadrature rule for the t -variable of sufficient degree to be sure that the integral has been determined to machine precision. We compute one thousand samples of the vector \mathbf{a} and report the maximal errors. Comparisons of two different quadrature rules always involve the same \mathbf{a} -vectors.

When $\Omega = T_2$ the standard approach is to approximate the transformed integral using the rule (16). Here we compare this rule with the cubature rules of table 1. This is equivalent to comparing the initial quadrature rule with the final rule in the node elimination process. The results are shown in figure 3, where the left plot shows the error versus the degree, and the right plot shows the error versus the number of nodes.

For higher dimensional simplices, the standard approach is to use the Duffy transform and use tensor product Gauss-Jacobi rules. The plots 4 and 5 compare the quadrature error of these rules with the rules of tables 2 and 3.

One can see that for the simplices the accuracy of the tensor product and the newly obtained rules of the same degree are very similar. This is despite the fact that the tensor product rules integrate polynomials in the space $\{\mathbf{x}^\alpha : \alpha_i \leq p\}$ exactly, which is a much larger space than \mathbb{P}_p^d . Apparently, these additional polynomials do not contribute to the accuracy in our examples. The right figure shows the same data, but here the error is plotted versus the number of quadrature nodes. This illustrates that the rules obtained with the elimination process require much fewer function evaluations to achieve the same accuracy. The gain of using these rules increases with the dimension.

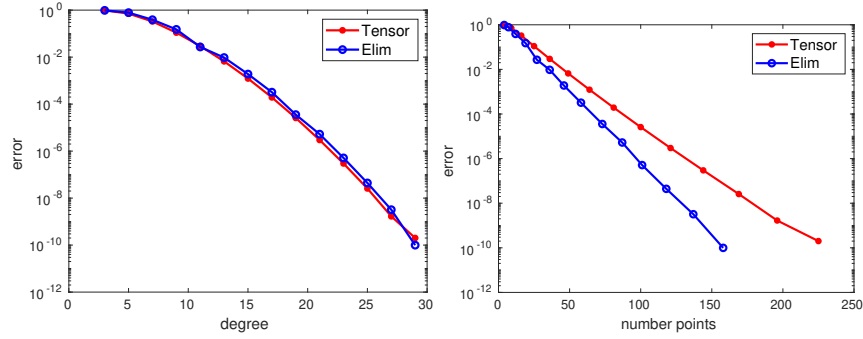


Figure 3: Comparison of the tensor product rules with the rules of table 1. $\Omega = T_2$. Left: error vs. degree. Right: error vs. number points.

The obvious approach for the domain $T_2 \times T_2$ is to use the quadrature rule in (16) for both triangles. Alternatively, one can use the rules of table 3. The resulting cubature errors are shown in figure 5.

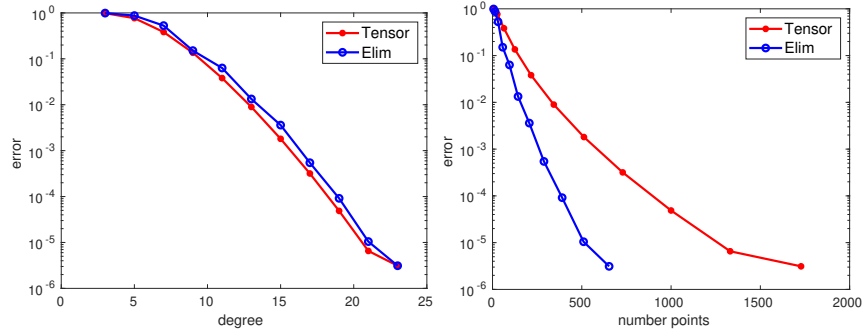


Figure 4: Comparison of the tensor product rules with the rules of table 2. $\Omega = T_3$. Left: error vs. degree. Right: error vs. number points.

Here it is interesting that for the same degree the tensor product rule is more accurate but the generalized Gauss rule is much more accurate for the same number of cubature nodes.

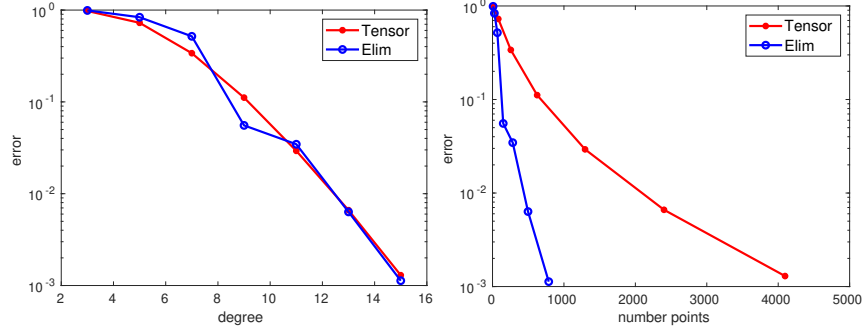


Figure 5: Comparison of the tensor product rules with the rules of table 3. $\Omega = T_4$. Left: error vs. degree. Right: error vs. number points.

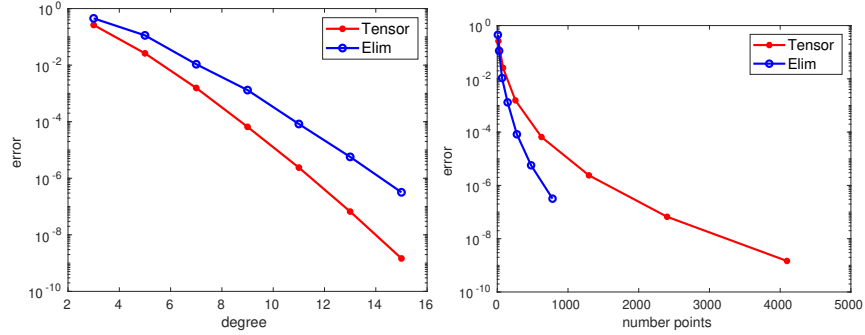


Figure 6: Comparison of the tensor product rules with the rules of table 4.

6. Conclusions

We have developed a new node elimination scheme, implemented it for several high-dimensional polytopes and obtained high-degree cubature rules. In the node elimination the degree of precision of a cubature rule is preserved while the number of nodes is reduced. For the integrands considered here, the node elimination does not reduce the accuracy in the case that the domain is a simplex, while for $T_2 \times T_2$ the accuracy is somewhat reduced. However, in all cases the trade off between cost in terms of evaluation points and accuracy is greatly improved with the newly obtained rules. Why two cubature rules of the same

degree of precision can have different accuracies appears to be an open research question.

It is well known that symmetries of the domain can be exploited to reduce the number of unknowns of the moment equations. This is of practical importance for domains in higher dimensions than what is presented in this work. However, this also gets more difficult because of the more complicated structure of the symmetry group of high dimensional polytopes. This is another area where further development of the method is needed.

References

- [1] E. L. Allgower and K. Georg. *An Introduction to Numerical Continuation Methods*. Classics in Applied Mathematics. SIAM, 2003.
- [2] I. Babuška. The p- and hp-versions of the finite element method: the state of the art. In M. Y. Hussaini D. L. Dwoyer and R. G. Voigt, editors, *Finite Elements: Theory and Applications*. Springer, 1988.
- [3] A. Bonito, W. Lei, and J. E. Pasciak. Numerical approximation of the integral fractional Laplacian. *Numerische Mathematik*, 142:235–278, 2019.
- [4] R. Cools. Constructing cubature formulae: the science behind the art. *Acta Numerica*, pages 1–54, 1997.
- [5] R. Cools. An encyclopaedia of cubature formulas. *J. Complexity*, 19:445–453, 2003.
- [6] D. A. Dunavant. High degree efficient symmetrical Gaussian quadrature rules for the triangle. *Internat. J. Numer. Methods Engrg.*, 21:1129–1148, 1985.
- [7] M. Gentile, A. Sommariva, and M. Vianello. Polynomial interpolation and cubature over polygons. *J. Comput. Appl. Math.*, 235(17):5232–5239, 2011.
- [8] J. Jaśkowiec and N. Sukumar. High-order cubature rules for tetrahedra. *Internat. J. Numer. Methods Engrg.*, 121:2418–2436, 2020.
- [9] V. Keshavarzzadeh, R. Kirby, and A. Narayan. Numerical integration in multiple dimensions with designed quadrature. *SIAM J. Numer. Anal.*, 40(4):A2033–A2061, 2018.
- [10] T. Koornwinder. Two-variable analogues of the classical orthogonal polynomials. In R.A. Askey, editor, *Theory and Applications of Special Functions*, pages 435–495. Academic Press, 1975.
- [11] N. Manson and J. Tausch. Quadrature for parabolic Galerkin BEM with moving surfaces. *Comput. Math. Appl.*, 77(1):1–14, 2019.

- [12] S.-A. Papanicolopoulos. Computation of moderate-degree fully-symmetric cubature rules on the triangle using symmetric polynomials and algebraic solving. *Comput. Math. Appl.*, 69:650–666, 2015.
- [13] S. Sauter and C. Schwab. *Boundary Element Methods*. Springer, 2011.
- [14] A. Slobodkins. gen-quad, <https://github.com/arkslobodkins/gen-quad>.
- [15] A. H. Stroud. *Approximate Calculation of Multiple Integrals*. Prentice-Hall, 1971.
- [16] Y. Sudhakar, A. Sommariva, M. Vianello and W. A. Wall. On the use of compressed polyhedral quadrature formulas in embedded interface methods. *SIAM J. Sci. Comput.*, 39(3), 2017.
- [17] J. Tausch. Adaptive quadrature rules for Galerkin BEM. *Computers Math. Appl.*, 113:270–281, 2022.
- [18] B. Vioreanu and V. Rokhlin. Spectra of multiplication operators as a numerical tool. *SIAM J. Sci. Comput.*, 36(1):A267–A288, 2014.
- [19] H. Xiao and Z. Gimbutas. A numerical algorithm for the construction of efficient quadrature rules in two and higher dimensions. *Comput. Math. Appl.*, 59(2):663–676, 2010.